Electronic supplementary information (ESI) for

New Surfactant-Copper(II) Complex Based on 1,4-Diazabicyclo[2.2.2]octane Amphiphile. Crystal Structure Determination, Self-Assembly and Functional Activity

*Elena P. Zhiltsova,[a] Tatiana N. Pashirova,[a] Marina R. Ibatullina,[a] Svetlana S. Lukashenko,[a] Aidar T. Gubaidullin,[a] Daut R. Islamov,[b] Olga N. Kataeva,[a] Marianna P. Kutyreva,[b] and Lucia Y. Zakharova,[*a]*

[a]Arbuzov Institute of Organic and Physical Chemistry, FRC Kazan Scientific Center of RAS, Arbuzov str., 8 Kazan, 420088, Russian Federation

[b]Kazan (Volga Region) Federal University, 18, Kremlevskaya str., Kazan 420008, Russian Federation

* Lucia Ya. Zakharova, Arbuzov Institute of Organic and Physical Chemistry, FRC Kazan Scientific Center of RAS, Arbuzov St. 8, Kazan, 420088, Russian Federation, E-mail: lucia@iopc.ru; luciaz@mail.ru

Contents

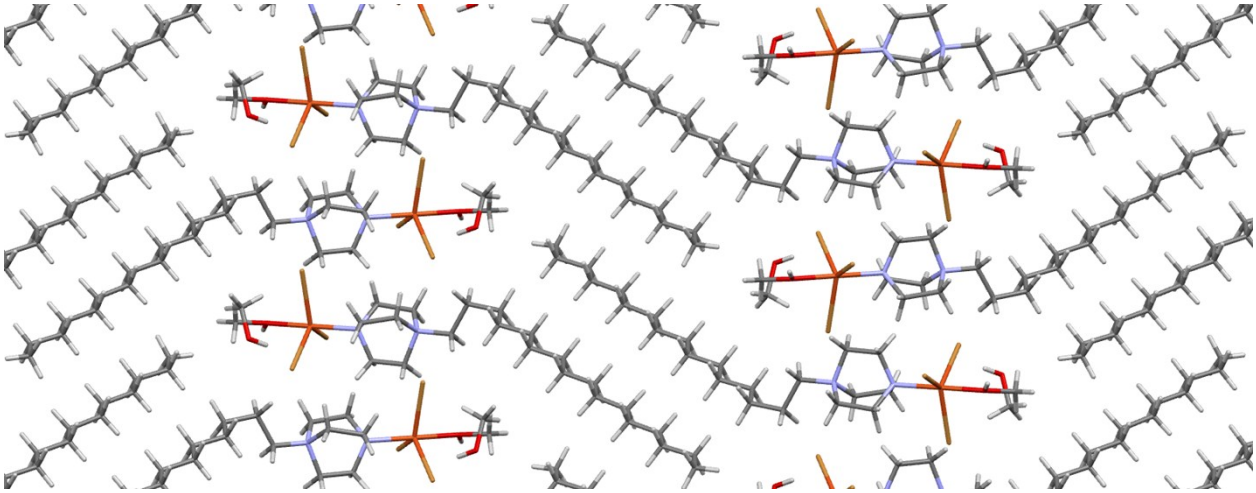

Figure S1. A fragment of crystal packing of complex [Cu(L)Br_3].

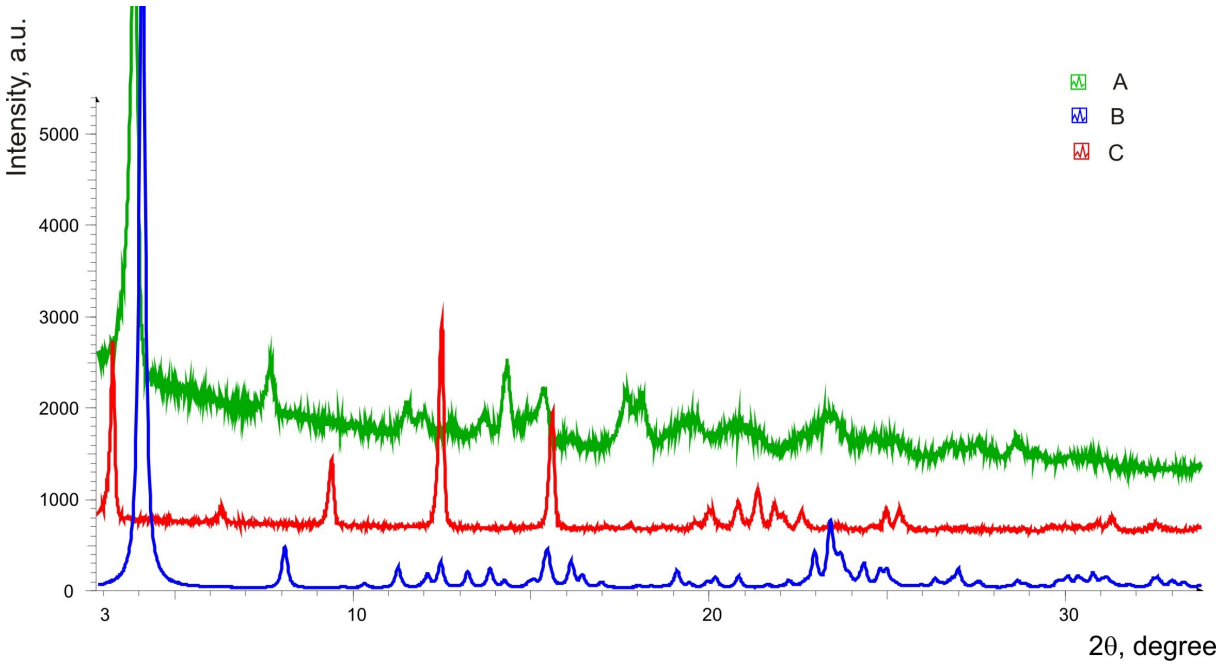

Figure S2. Experimental X-ray powder patterns for the dried sample of [Cu(L)Br_3] complex (curve A) at room temperature and polycrystalline ligand (LBr) (curve C). At the bottom (curve B) - theoretical XRD curve for methanol complex [[Cu(L)Br_3]×MeOH] calculated on the basis of the unit cell parameters and coordinates of the atoms.

Spectral and color characteristics of $[Cu(L)Br_3]$ complex, LBr - $CuBr_2$ mixture and CQBr- $CuBr_2$ mixture

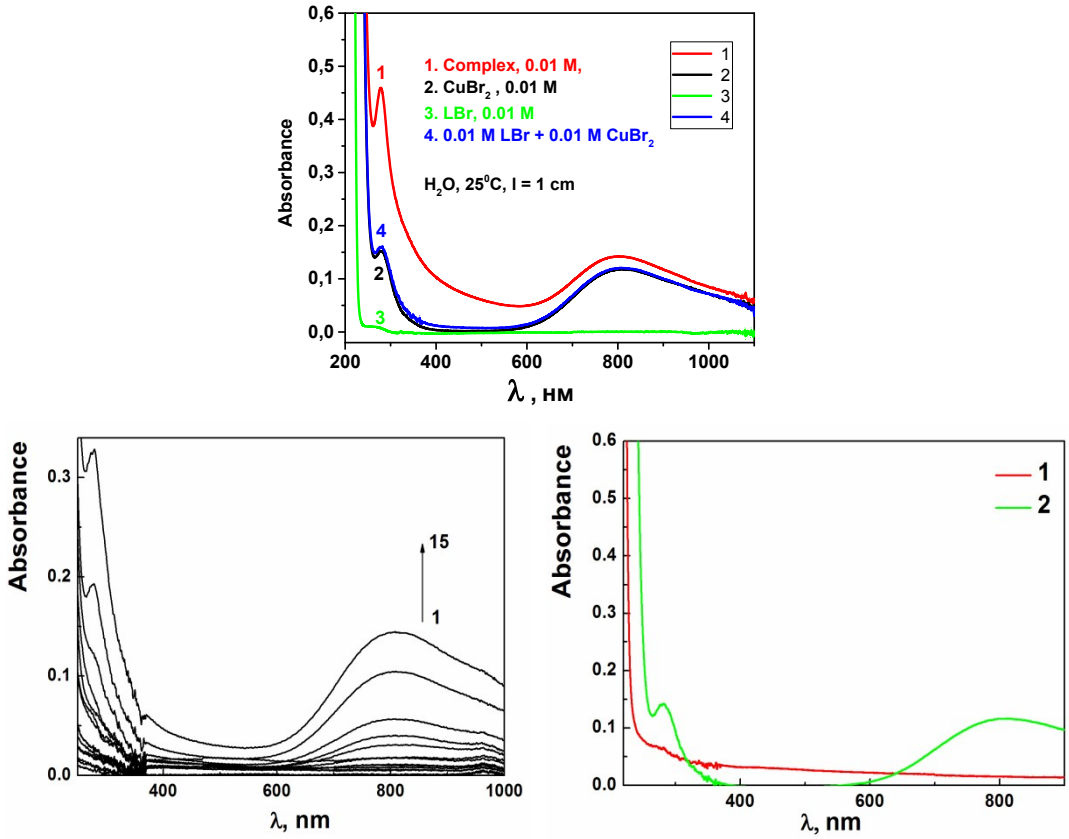

Figure S3. Absorption spectrum of $[Cu(L)Br_3]$ complex (*1*), $CuBr_2$ (*2*), LBr (*3*), LBr - $CuBr_2$ mixture (1:1) (*4*) in water, $C_{complex} = C_{CuBr2} = C_{LBr} = 0.01$ M, l = 1 cm, 25 ºC.

Figure S4. Absorption spectrum of solutions of cetylquinuclidinium bromide (CQBr) in presence $CuBr_2$ in water, c_{CQBr} (mM) = c_{CuBr2} = 0.02 (*1*), 0.04 (*2*), 0.06 (*3*), 0.08 (*4*), 0.1 (*5*), 0.2 (*6*), 0.4 (*7*), 0.6 (*8*), 0.8 (*9*), 1 (*10*), 2 (*11*), 3 (*12*), 4 (*13*), 8 (*14*), 10 (*15*); l = 1 cm, 40 ºC.

Figure S5. Absorption spectrum of solutions of cetylquinuclidinium bromide (CQBr) (*1*), $CuBr_2$ (*2*) in water, $c_{CQBr} = c_{CuBr2}$ = 10 mM, l = 1 cm, 40 ºC.

This work is not focused on the mechanism of interaction LBr and $CuBr_2$ in different media, except for methanol, which was used as reaction medium. In the latter case the donor-acceptor mechanism was unambiguously proved (X-ray analysis). The involvement of ionic interactions in the case surfactants with quaternized nitrogen (CTAB, CQBr) does not except the contribution of the donor-acceptor mechanism in the case of LBr.

Nevertheless, we carried out examination of the color of solutions (Figure A). As can be seen the color of all surfactant-salt mixtures and complex is green within the first 15 min tested. However different color behavior occurs in course of time. Samples became colorless in the case of CTAB and CQBr, while remained green for 2 hours in the case of LBr and $[Cu(L)Br_3]$. No changes occur in methanol.

These data make it possible to conclude that two different mechanisms can be involved in the surfactant-salt interaction: electrostatic interactions are important for classical surfactants (CTAB, CQBr), while donor-acceptor mechanism occurs in the case of DABCO systems involving tertiary nitrogen. The latter mechanism was supported by our earlier work [E.P. Zhil'tsova, et al. Complexation of 1-alkyl-4-aza-1-azoniabicyclo[2.2.2]octane bromides with transition metal cations in acetone, Liquid Crystals and their Application, 2015, **15** (4), 48–55], devoted to the complex formation in the LBr – $CuBr_2$ system in acetone, in which the stable complex M : L = 3 : 2 was observed.

In 15 min, in acetone

In 2 hours, in acetone

In time, in methanol

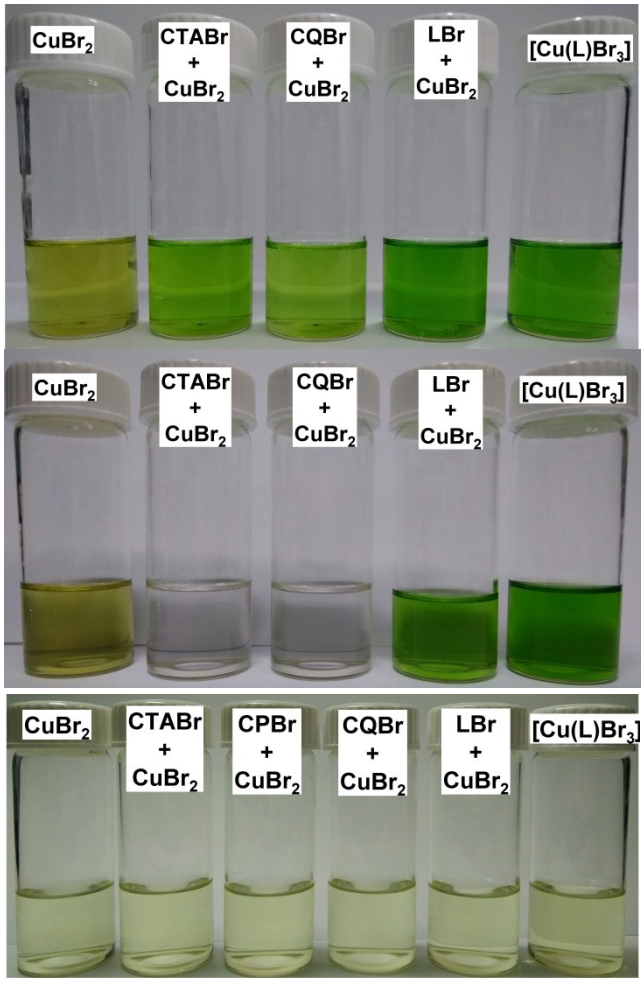

Figure A. Visualization of the color of samples (solution of salt, surfactant-salt binary mixtures and complexes) in acetone and methanol.

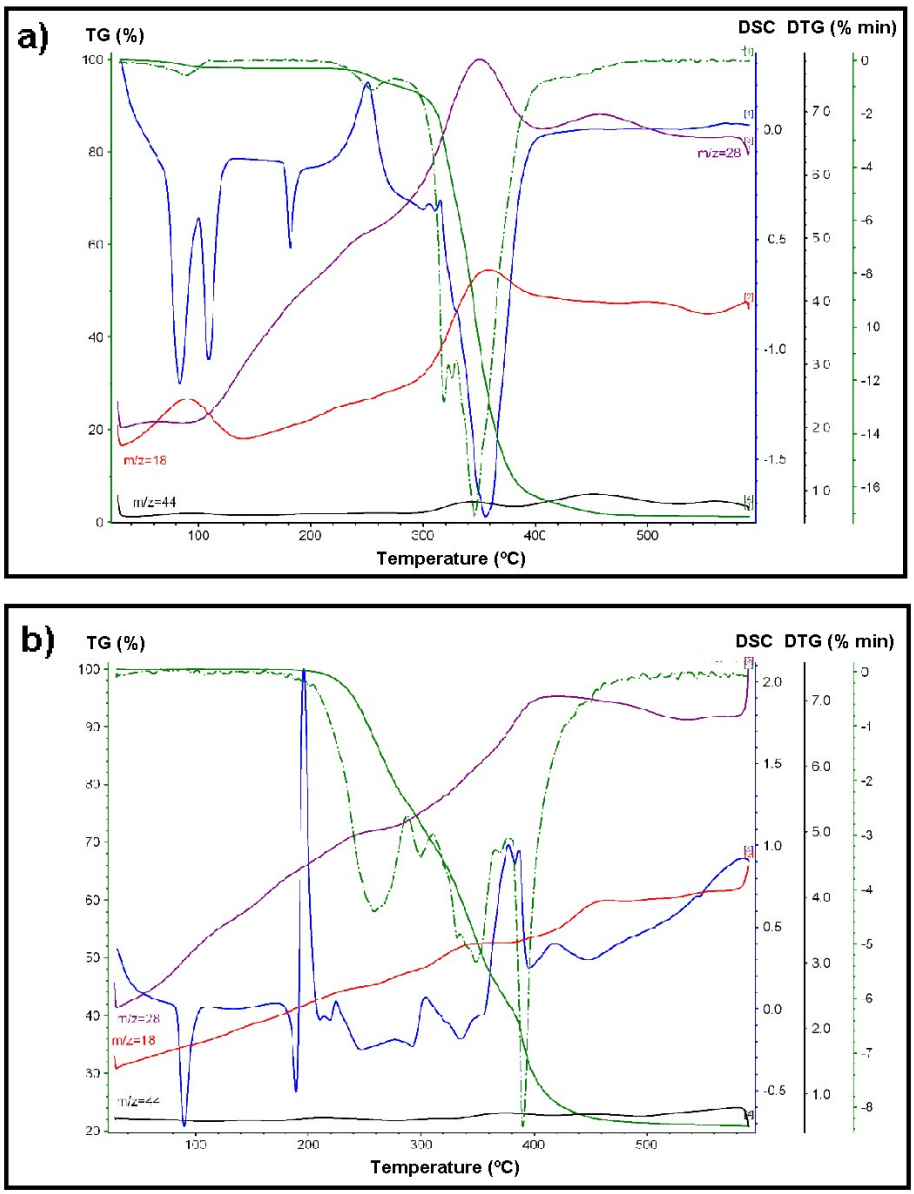

Figure S6. Derivatogram of LBr (a), [Cu(L)Br_3] complex (b).

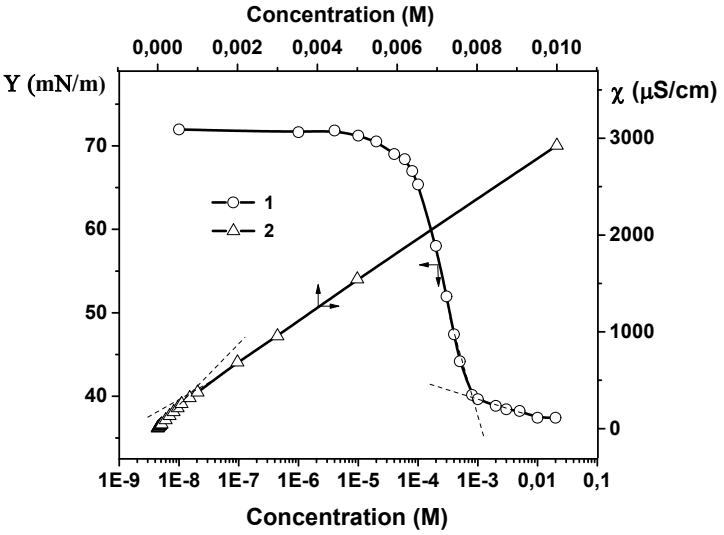

Figure S7. Dependence of surface tension (*1*) and specific electric conductivity (*2*) of aqueous solutions of LBr - $CuBr_2$ mixture (1:1) on concentration of surfactant, 25 ºC.

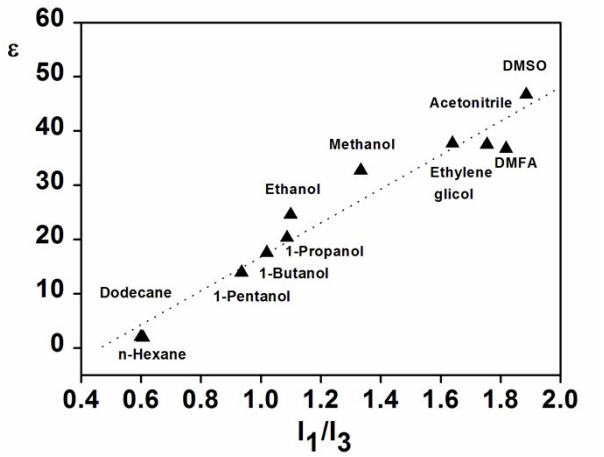

Figure S8. I_1/I_3 ratio of pyrene in nonaqueous media with various dielectric permittivities (according to the data from[1]).

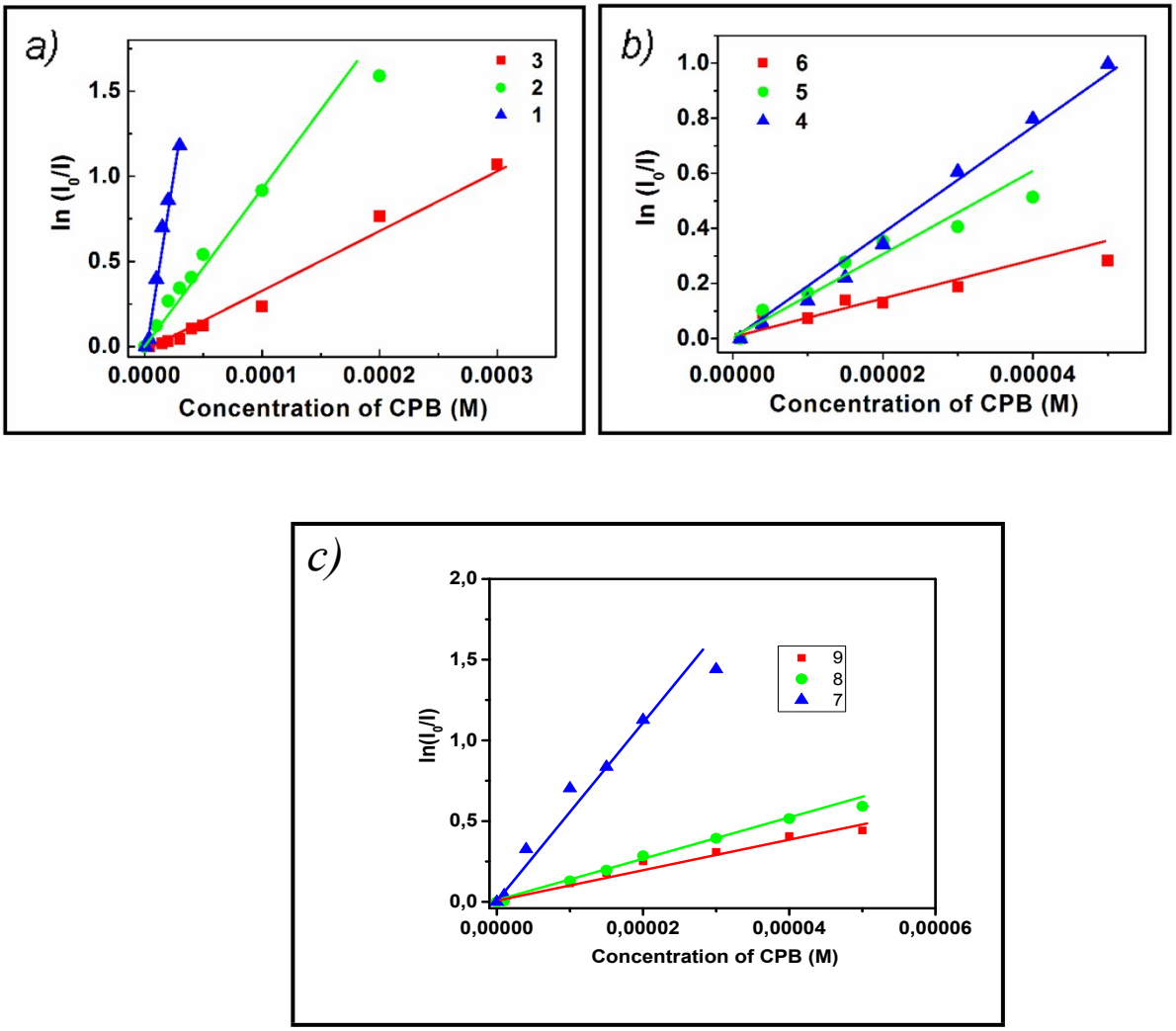

Figure S9. Dependence of ln (I_0/I) in the solutions of [Cu(L)Br_3] complex (*a*), LBr (*b*) and LBr – $CuBr_2$ (1:1) mixture (*c*) on the concentration of CPB at $C_{complex}$ (M) 0.001 (*1,7*), 0.004 (*2,5,8*), 0.008 (*3,6,9*), 0.002 M (*4*), λ = 395 nm (*1-5, 7-9*), 384 nm (*6*).

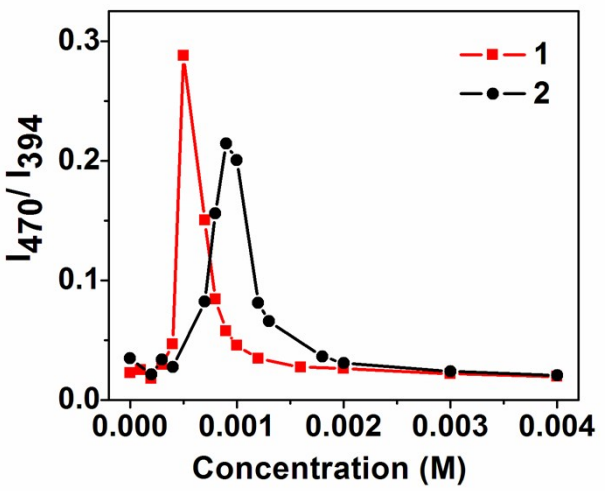

Figure S10. Dependence of excimerization coefficient of pyrene on the concentration of metallosurfactant [Cu(L)Br_3] (*1*) and LBr (*2*) in water, $\lambda_{excitation}$ = 335 нм, C_{pyrene} = 1×10^{-6} M, 25 ^{o}C.

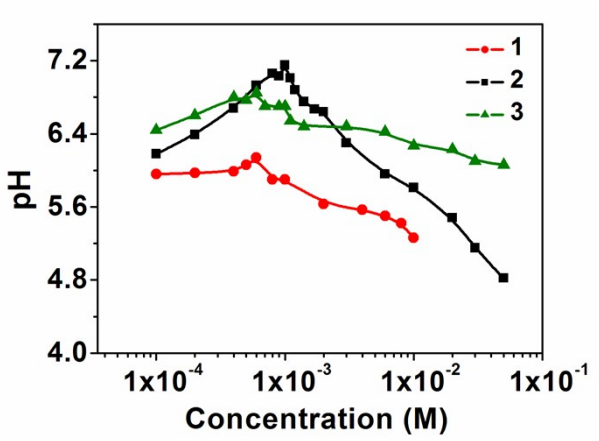

Figure S11. Dependence of pH of aqueous solutions of [Cu(L)Br_3] (*1*), LBr (*2*), and CTAB (*3*) on their concentration.

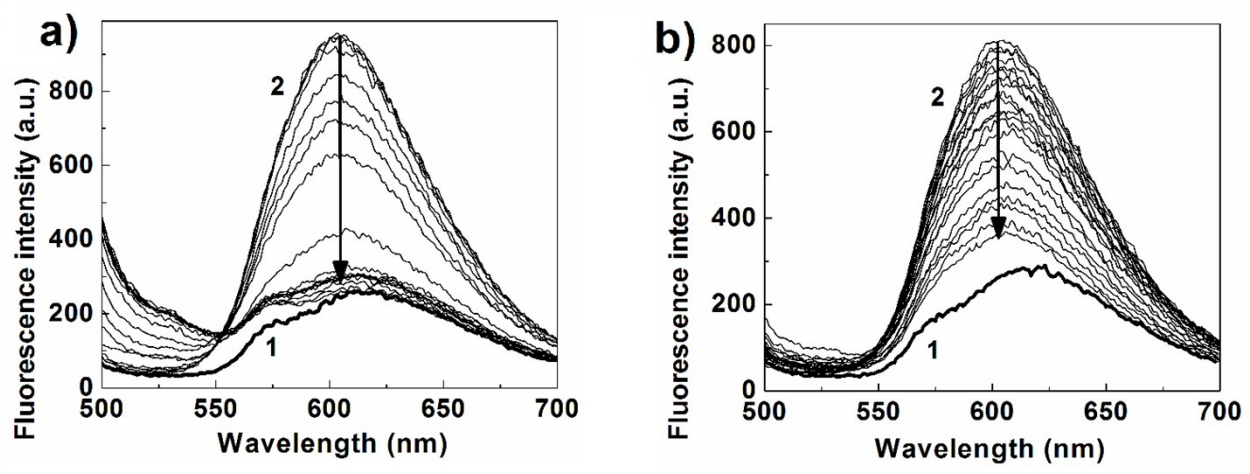

Figure S12. Fluorescence emission spectra of free (1) and bound EB (ONu/EtBr) containing different amounts of [Cu(L)Br_3] (a) $CuBr_2$ (b) the down arrows indicate the increment of molar ratio *r*

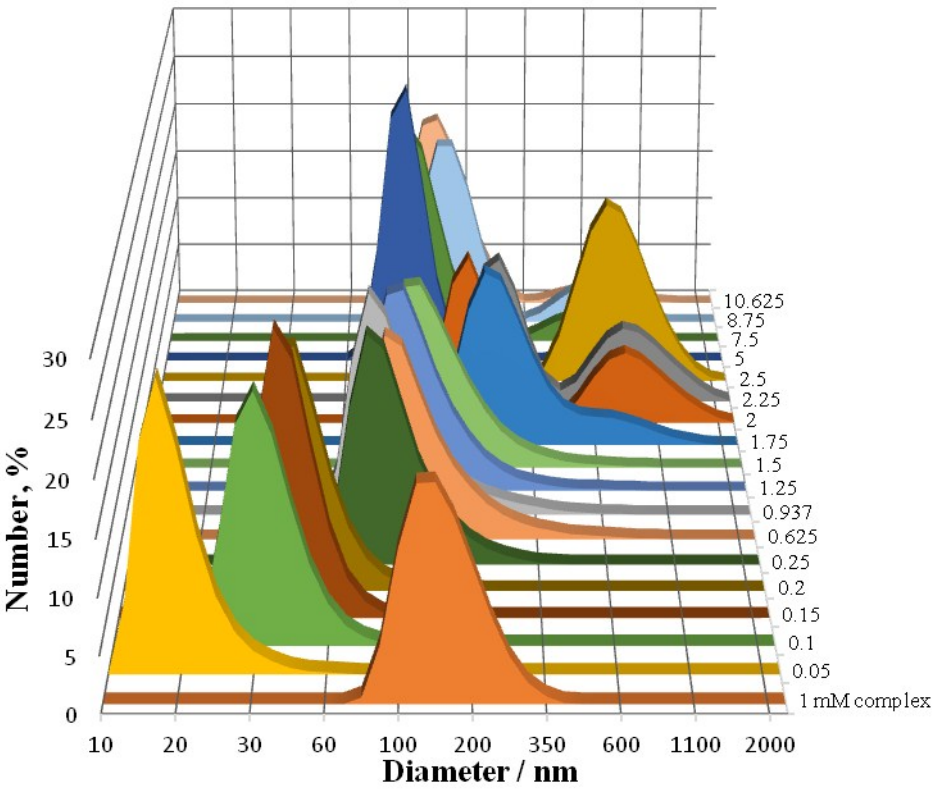

Figure S13. Size of $[Cu(L)Br_3]$/ONu complexes versus charge ratio r(±) plot for metallsurfactant/ONu binary systems, 25 ºC.

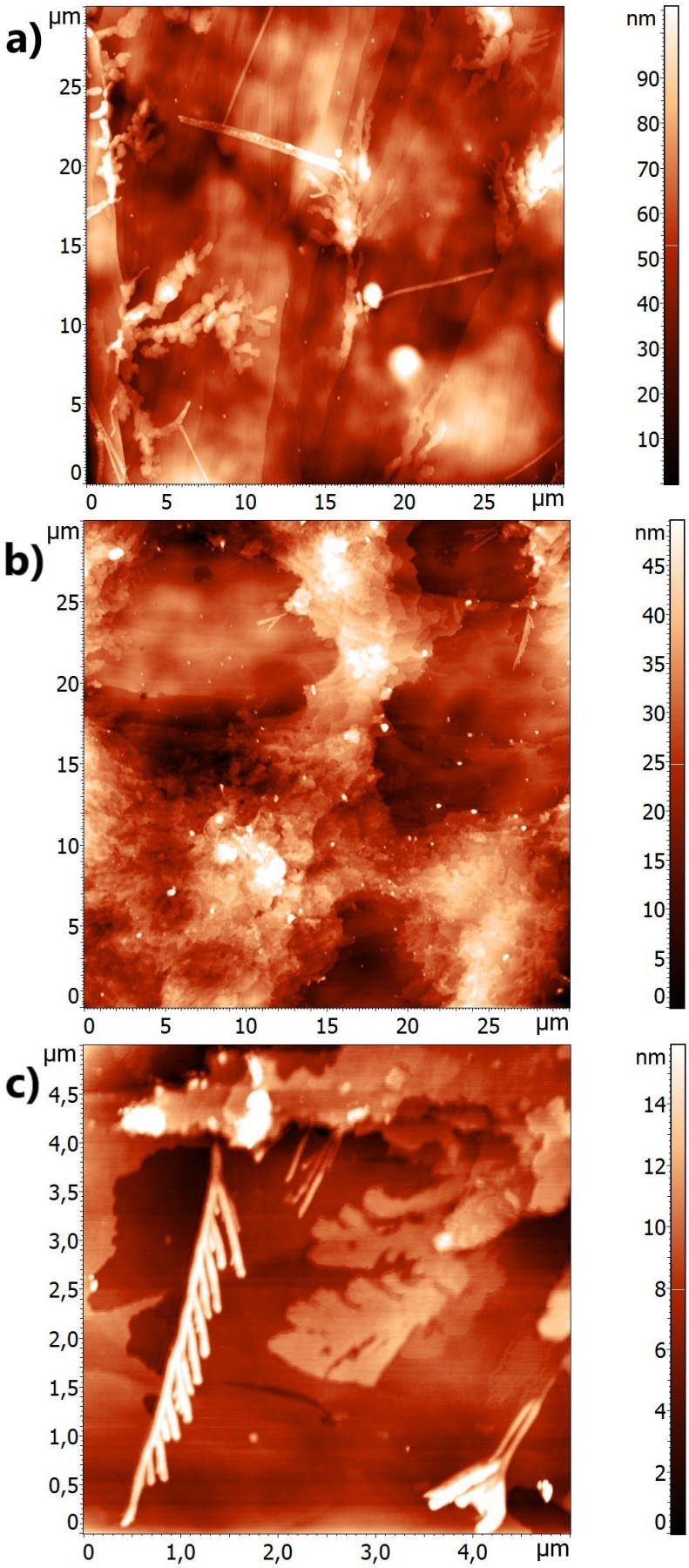

Figure S14. AFM image of particles of LBr (a), [Cu(L)Br_3] complex (b) on a highly oriented pyrolytic graphite (HOPG) and an enlarged AFM image of the [Cu(L)Br_3] complex fractal structures (c).

The surface morphology of thin films of the LBr ligand and its complex with copper deposited from the aqueous solution on the highly oriented pyrolytic graphite (HOPG) surface was characterized by atomic force microscopy. There are two types of nanoformations on the ligand LBr thin film: i) fractal formations 3.5-10 μm in length, about 1 micron in width at the base and 40-80 nm in height, and ii) extended nanowires of about 11 μm in length, 200-400 nm in width and about 60 nm in height, presumably collected from bundles of cylindrical micelles.

For the [Cu(L)Br_3] complex, i) fractal-branched structures 2-4 μm in length, 100-1200 nm in width and 4-10 nm in height are also observed. However, there are also ii) clusters of flat islands layered each other, with the height of each island 2-5 nm, and iii) spherical nanoparticles with a diameter of 350-550 nm and a height of about 50 nm.

References

(1) K. Kalyanasundaran, J. K. Thomas, *J. Amer. Chem. Soc.,* 1977, **99**, 2039-2044.